ACS OMEGA

http://pubs.acs.org/journal/acsodf

Article

Enhancement Mechanism of Minerals on Lignite−Water Molecule Interactions

Ying Yue Teng, Shi Rui Han, Yue Yin Song,* Xue Bai, and Yin Min Song

Cite This: *ACS Omega* 2023, 8, 9111−9120

Read Online

ACCESS | Metrics & More | Article Recommendations

ABSTRACT: Five coal samples were prepared by deashing Shengli lignite in distinct phases, which consisted of residual ash from spontaneous combustion. The effects of removal and introduction of inherent minerals on the water reabsorption performance of coal samples were systematically investigated in three aspects: pore structure, oxygen-containing functional groups, and lignite materials. Low-field nuclear magnetic resonance spectroscopy was employed to investigate the changes in the water molecular adsorption tendency of coal samples with the variation in the mineral content. The study elucidates that the hygroscopic performance of the coal samples is significantly reduced due to the massive removal of inherent minerals. However, the pore structure of the coal samples after HCl/HF washing becomes more developed, and the oxygen-containing functional groups on the surface are more exposed, leading to an increase in the equilibrium adsorbed moisture content (EMC) of the coal samples. The binding force between coal samples and water molecules is reduced by the removal of the inherent minerals, which weakens the interaction forces between lignite and water molecules. The oxygen-containing functional groups on the surface of lignite interact with the residual ash from spontaneous combustion to enhance the binding force between lignite and surface water molecules, thus leading to the improved tendency of lignite to adsorb water molecules. The formation of intermediate complexes between minerals and oxygen-containing functional groups, in particular, carboxyl functional groups, on the surface of lignite enhances the acting force of polar sites, which improves the interaction of lignite−water molecules.

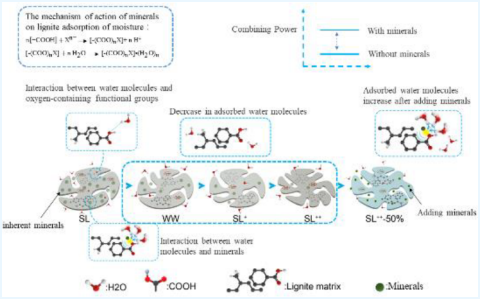

1. INTRODUCTION

Clean coal utilization is becoming extensively crucial with the economic development at the global scale, and the availability of energy is becoming immensely constrained. China has abundant coal resources, ranging from lignite to anthracite, but their quantity and distribution are extremely uneven. Among them, more than 50% of the country's total coal resources include lignite and low-metamorphic bituminous coal.[1] Currently, more than 90% of the refined lignite in China is used to generate electricity via combustion.[2] Lignite contains a high concentration of oxygen-containing functional groups, a complex pore structure, and a large number of mineral ions, resulting in its high water content and higher sensitivity to spontaneous combustion. After upgrading, lignite becomes more prone to absorb water, which reduces its calorific value and increases its storage and transportation costs,[3−5] causing substantial safety and economic problems for coal-related industries.[6]

In past decades, extensive research efforts have been devoted to research on the resorption of lignite. In lignite, the energy level of the free water and pore water is the lowest, and the binding ability of water to coal is extremely weak. Therefore, water in lignite is extremely facile to vaporization and readsorption, which is critical for lignite dehydration.[7−9] Many factors influence lignite water resorption. The reabsorption of lignite moisture is intimately connected with the oxygen-containing functional groups on its surface.[10] The hydrophilicity sequence of these functional groups is as follows: carboxyl group > phenolic hydroxyl group > carbonyl group > methoxy group. The dehydration energy of samples with more carboxyl groups is lower than that of samples with more phenolic hydroxyl groups.[11−15] It has been verified that increasing the ether bond content in lignite leads to a significant enhancement in the water adsorption capacity, and the ether bonding can cause water molecules to form a stable adsorption monolayer of water.[16] Moisture resorption is also influenced by the pore structure of lignite. During the drying and upgrading of lignite, the specific surface area and total volume of lignite increase; however, the gelatinous structure shrinks and collapses significantly, reducing the hydrophilicity of dehydrated lignite, therefore, restricting water reabsorption.[17,18] The mineral composition of lignite also contributes

Received: September 6, 2022
Accepted: February 9, 2023
Published: March 6, 2023

https://doi.org/10.1021/acsomega.2c05786
ACS Omega 2023, 8, 9111−9120

significantly to its high water content. Gosiewska et al.[19] observed that the minerals in coal exhibited comparatively high hydrophilicity, which increased with mineral concentration and size. According to the literature,[20,21] quartz, kaolinite, muscovite, gypsum, orthoclase, and hematite are the predominant discrete minerals in Shengli lignite. Moreover, it was considered that when discrete minerals were removed, the ionic cross-linking force and ionic hydration gradually decreased, resulting in an obvious decline in the moisture absorption capacity of lignite. Fei et al.[22] investigated the changes in the equilibrium resorption water content of six types of Victorian lignite after water and acid washing at different relative vapor pressures and revealed that the presence of inorganic cations increased the equilibrium adsorbed moisture content (EMC) value in Victorian lignites. Liu et al.[23] demonstrated that Shengli lignite was loaded with metal ions after acid demineralization treatment, and metal loading increased with the increase in the metal ion concentration. The EMC of ion exchange samples increased with increasing ion loading due to metal ion hydration.

Currently, numerous factors impacting lignite moisture resorption are controversial, and no efficient approach to restrict lignite moisture resorption has been developed. Moreover, lignite is extremely flammable, and the ash from spontaneous combustion gets deposited on its surface. The impact of additional minerals on the moisture absorption tendency of lignite is currently unpredictable. Therefore, this research employed Shengli lignite as the research object and developed five coal samples via a step-by-step acid washing process, which contained spontaneous combustion residual ash to evaluate the moisture adsorption performance. Nitrogen adsorption experiments, infrared (FT-IR) spectroscopy, X-ray diffraction (XRD), X-ray photoelectron spectroscopy (XPS), and other methods were used to characterize the changes in pore structure, functional groups, and mineral content of treated coal samples, while low-field nuclear magnetic resonance (NMR) spectroscopy was used to analyze the force and water content of coal samples adsorbing water molecules. The objective of this research is to explore the impact of inherent and extrinsic minerals on the moisture adsorption properties of lignite and to investigate the mechanism of minerals on the lignite−moisture interaction.

2. EXPERIMENTAL SECTION

2.1. Materials. The lignite from the Shengli coalfield in the Xilin Gol League, Inner Mongolia, China, was selected as the research object. The Shengli lignite was crushed and sieved using a ball mill and a standard sieve. Coal samples with a mesh size of 200−400 were selected and dried at 105 °C for 4 h in a blast dryer. The Shengli coal samples utilized in the experiments were procured and labeled as SL.

2.2. Preparation of Coal Samples. In a beaker, raw coal and deionized water were mixed in a 1 g:10 mL ratio and stirred at room temperature for 24 h followed by filtration. The residue after filtration was washed several times with deionized water, separated through a suction filter, and subsequently dried at 105 °C for 4 h. The resulting product was designated as WW.

Next, concentrated hydrochloric acid (38 wt %) was diluted with water in a 1 mL:1 mL volume ratio, which was then mixed with the SL sample in a 1 g:10 mL ratio and stirred at room temperature for 24 h. The resulting solid−liquid mixture was then suction filtered and washed with distilled water until there was no Cl^-. A demineralized coal sample, named SL^+, was obtained after drying at 105 °C for 4 h.

SL^+ and HF were mixed in a ratio of 1 g:3 mL, maintained, and stirred gently for 30 °C, 24 h to completely dissolve the coal sample in a hydrofluoric acid solution. Then, the mixture was allowed to stay for precipitation till the liquid−solid phase stratification occurred. After the supernatant was removed, it was repeatedly washed to render it free of F^-. $CaCl_2$ was employed for the detection of F^- present in the solution since CaF_2 would precipitate in the presence of F^-. After making the mixture F^- free, the solid coal sample was collected via suction filtration followed by drying and was designated as SL^{+2}.

The residual ash after spontaneous combustion of lignite was weighed and mixed with deionized water according to the SL ash percentage in industrial analysis. The mixture was stirred at room temperature for 12 h followed by the addition of SL^{+2}, and the stirring was continued for 24 h. The coal sample obtained by suction filtration and drying was named as SL^{+2}-50%.

2.3. Moisture Adsorption Experiments. Lithium chloride and potassium chloride were selected as solutes based on the comparison table of humidity in different salt solutions and the solubility table such that the weighed amount of the solutes was greater by 30% than their solubility at 30 °C. The saturated salt solution with a humidity of 43% and 83% was prepared by adding deionized water (2000 mL). The coal sample was placed in a 40-mm weighing bottle, which was covered and weighed as m_0. It was then placed in a desiccator after removing its cap. A series of saturated salt solutions was deposited sequentially beneath the desiccator, and the desiccator was placed at a constant temperature of 30 °C. At regular time intervals, the weighing bottle was retrieved, covered, and weighed as m_t. If the difference between the two adjacent weighing values was ≤ 0.001 g, the resorption was regarded to achieve equilibrium. The water adsorption capacity and equilibrium adsorption rate are calculated as follows:

$$\text{adsorption capacity} = m_t - m_0 \tag{1}$$

$$\text{EMC} = \frac{m_t - m_0}{m_0} \times 100\% \tag{2}$$

2.4. Analysis Methods. *2.4.1. X-ray Diffraction.* The minerals and crystal structures in the test samples were investigated by XRD using an X-ray diffractometer (Rigaku, Japan, SmartLab 9KW) with Cu target configuration and high-sensitivity D/teX Ultra 250 detection system. The scanning range was 5−90°, with a scanning speed of 2°/min.

2.4.2. Infrared Spectroscopy. The oxygen-containing functional groups were examined by Fourier transform infrared (FTIR, NEXUS670, American Nicolet Corporation) spectroscopy. The dried sample and KBr were homogenized uniformly at a mass ratio of 1:100. The following were the test conditions: the scanning wavelength range of 400−4000 cm^{-1}, with a scanning time of 20 s. The resolution and wavenumber accuracies were 0.125 and 0.001 cm^{-1}, respectively.

2.4.3. Low-Temperature Nitrogen Adsorption Method. The pore structure parameters of the samples were evaluated and analyzed employing a fully automatic surface area and pore analyzer (Autosorb-iQ type, Quanta Corporation, United States). A filling sample of coal (~0.5 g) was acquired, the degassing temperature was set to 200 °C, and the time was set to 6 h. It was refilled with N_2 after degassing, and then weighed

https://doi.org/10.1021/acsomega.2c05786
ACS Omega 2023, 8, 9111−9120

and recorded after cooling. The Brunauer−Emmett−Teller (BET) and Barrett−Joyner−Halenda (BJH) methods were employed to estimate the specific surface area, pore volume, and pore distribution of each sample.

2.4.4. X-ray Photoelectron Spectroscopy. X-ray photoelectron spectroscopy (XPS) was performed using an ESCALAB250Xi spectrometer (Thermo-Fisher Company, United States). The vacuum level was 3×10^{-7} Pa, the scanning area was 300×300 μm^2, and it was calibrated with C1s (284.8 eV) standard. The binding energy (BE) was represented by the abscissa in the XPS spectrum, while the electron count was represented by the ordinate.

2.4.5. Low-Field NMR Spectroscopy. The water content of the samples was determined by ^1H NMR spectroscopy (VTMR20-010V-T, Shanghai Niumag). The NMR analysis software was used to collect signal values and determine the transverse relaxation time T_2 in the Carr−Purcell−Meiboom−Gill (CPMG) sequences of the test samples. Three signals were recorded for each sample, and the results were averaged. The test parameters included a resonance frequency of 21.306 MHz, a magnetic intensity of 0.5 T, a coil diameter of 25 mm, a magnetic temperature of 35.0 °C, and a sealing test. The coal sample (0.5−1 g) was placed in the detection oven, and the detection limit for water was 10 mg. The coal sample was placed in a specific humidity environment, and water was adsorbed on the surface of the lignite. Such coal samples were referred to as adsorbed water samples. The interaction strength between lignite and water molecules is expressed as the transverse relaxation time T_2 (ms) as follows:[16]

$$M_{xy} = M_0 \times \exp\left(\frac{-t}{T_2}\right) \quad (3)$$

where M_{xy} is the component of the macroscopic magnetization vector on the $x-y$ axis, M_0 is the initial magnetization vector, and T_2 is the transverse relaxation time. The interaction intensity M_{xy} is proportional to the relaxation time t, according to eq 3.

3. RESULTS AND DISCUSSION

3.1. Influence of Inherent Minerals on Lignite Moisture Resorption. *3.1.1. Resorption Curve of Demineralized Lignite.* Evaluation of moisture adsorption behavior of lignite is an important method for studying the interaction of lignite with water.[24] Shengli raw coal and gradually deashed coal samples were subjected to moisture resorption studies at 30 °C and relative humidity levels of 43% and 83%, respectively. Table 1 lists the numerical value of the EMC. The equilibrium adsorption water content of the four coal samples revealed the following pattern: $EMC_{SL} > EMC_{WW} > EMC_{SL++} > EMC_{SL+}$ when the relative humidity was 43% and 83%, respectively. This trend can be analyzed based on the changes in mineral content, oxygen-containing functional groups, and specific surface area in the coal samples. SL exhibited the strongest hygroscopic ability, and the EMC of SL, WW, and SL^{+2}, and SL^{+} were significantly different. In this study, the EMC of the same coal increased with an increase in relative humidity; the higher the relative humidity, the greater the EMC of the same coal.

Table 1. Equilibrium Adsorption Water Content (EMC) of Shengli Lignite and Its Deashed Coal Samples

	EMC/%	
sample	43%	83%
SL	7.73	13.89
WW	7.19	12.38
SL^{+}	5.29	9.45
SL^{+2}	6.04	10.69

3.1.2. Changes in Inherent Minerals. According to GB/T 212 2008, proximate analysis and ultimate analysis of all samples were performed using an industrial coal analyzer (5E-MAG6700) and elemental analyzer (Germany Elementar: VARIOEL Cube). The corresponding results are presented in Table 2. The mineral content of raw coal changed slightly after washing with water; however, after HCl, HCl/HF stepwise acid washing followed by demineralization, the mineral content reduced considerably, in particular, the ash content of the SL^{+2} coal sample, which was only 0.37. The volatile matter and fixed carbon content of coal samples changed slightly after stepwise acid washing and deashing. The mineral elements detected by ICP for all coal samples are presented in Table 3. Washing coal samples with water can only reduce the mass percent of Na and Ca in coal samples by 0.08% and 0.03%. After HCl stepwise acid washing, the metal elements in SL^{+} decreased by 1.5%, 0.08%, 0.4%, 0.51%, 0.05%, 0.58, and 0.06%.

Four different types of coal samples were scanned by the XRD technique to detect the changes in their composition and crystal structure after step-by-step demineralization, as illustrated in Figure 1. The crystal structure of the coal sample did not change considerably when it was washed with water and rinsed with HCl, and the diffraction peak intensities of kaolinite ($Al_4(OH)_8Si_4O_{10}$) and quartz (SiO_2) got marginally weakened. The minerals in coal samples were not entirely eluted by water washing and HCl. Diffraction peaks corresponding to minerals in coal samples disappeared completely after elution with HCl/HF.

3.1.3. Changes in Oxygen-Containing Functional Groups. The oxygen-containing functional groups on the coal surface influence lignite moisture resorption.[25] Figure 2 depicts the functional group changes in coal samples after different demineralization treatments. The region at 450−1200 cm^{-1} in the XRD patterns consists of distinct peaks corresponding to minerals in the coal sample. Herein, the difference between WW and SL was relatively small. This is attributed to the fact that the water washing led to the elution of only the surface minerals of coal samples; however, acid washing eliminated a portion of their inherent minerals. The peak intensity gradually decreased or even disappeared with the increase in the acid washing gradient. Among them, the peak at 449−634 cm^{-1} belonged to the bending vibrations of SiOSi, SiO, and organic sulfur.[26] The peak of SL^{+2} was significantly attenuated, indicating that HF eluted the majority of the Si-containing groups in the coal sample. The peaks of CO and COC were located between 1100−1300 cm^{-1}. Compared to SL, the peaks of SL^{+} and SL^{+2} were substantially enhanced. The peaks at 1740, 1705, and 1600 cm^{-1} corresponded to the aromatic C═O stretching vibration in coal; the C═O stretching vibration in alcohol, phenol, and a carboxylic acid; and the C═C stretching vibration peak of the aromatic skeleton, respectively. The stretching vibrations of SL^{+2} were significantly stronger than those of SL^{+} herein, with double peaks at 1740 and 1600 cm^{-1}, respectively, due to the exchange of metal ions in the carboxylate on the surface of lignite with H^{+} after leaching treatment to form carboxylic acid.[27] Simultaneously, it was

https://doi.org/10.1021/acsomega.2c05786
ACS Omega 2023, 8, 9111−9120

Table 2. Proximate Analysis and Ultimate analysis of Samples[a]

	proximate analysis (wt %)				ultimate analysis (wt %)				
sample/%	M_{ad}	A_d	V_d	FC_d	C	H	N	S	O[b]
SL	5.09	12.9	34.4	52.7	59.7	4.42	0.83	1.75	16.8
WW	2.99	9.76	40.7	49.5	60.5	3.97	0.86	1.09	21.1
SL^+	2.14	7.53	39.8	52.7	61.4	3.34	0.86	1.74	25.1
SL^{+2}	1.12	0.37	44.6	55.1	64.9	4.92	0.85	1.32	26.5

[a]Note: A: ash; V: volatile content; FC: fixed carbon; d: dried basis. [b]By difference.

Table 3. Metal Ion Percentage in Coal Samples

	coal based (wt %)						
samples	Al^{3+}	Fe^{n+}	Ca^{2+}	Mg^{2+}	K^+	Na^+	Mn^{n+}
SL	2.40	0.11	0.41	0.52	0.08	0.58	0.06
WW	2.40	0.11	0.38	0.43	0.08	0.50	0.06
SL^+	0.90	0.03	0.01	0.01	0.03	0.00	0.00
SL^{+2}	0.11	0.00	0.01	0.00	0.00	0.00	0.00

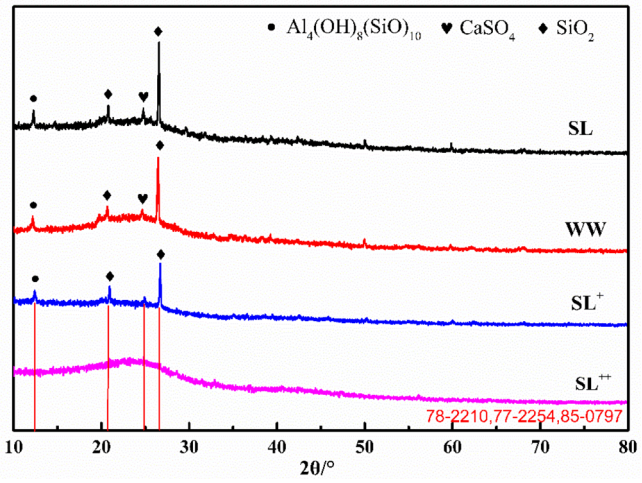

Figure 1. XRD patterns of Shengli lignite and deashed coal samples.

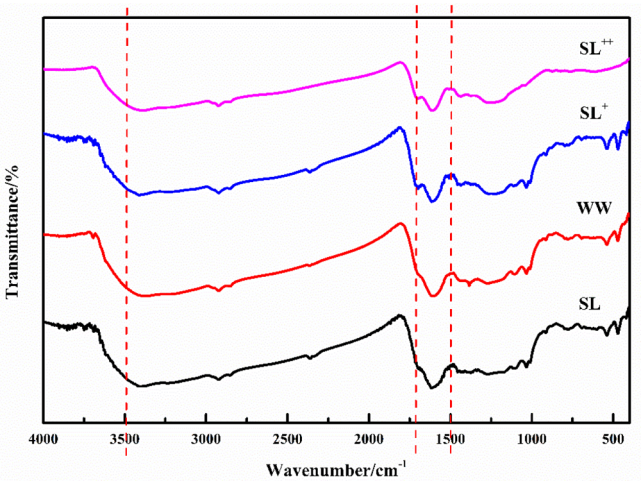

Figure 2. FTIR spectra of Shengli raw coal and deashed coal samples.

demonstrated that SL^{+2} contained fewer mineral ions. The C=C stretching vibration of the predominant aromatic hydrocarbon skeleton in the coal did not change appreciably, indicating that the main structure of the macromolecular skeleton of coal did not change after the acid treatment.

The XPS spectrum effectively depicts the occurrence state of different microscopic components and surface elements on the lignite surface. Figure 3(a) presents the C1s spectra of SL, WW, SL^+, and SL^{+2}, and Figure 3(b) shows the peak fitting of O1s spectra (Table 4). The C1s spectrum was divided into four peaks with distinct energies, in the order of low to high binding energy as follows: 284.8 eV of aromatic hydrocarbon (CC, CH), 284.56 eV of phenol or ether (CO), 286.63 eV of carbonyl (C = O), and 288.96 eV of a carboxyl group (COO). The oxygen-containing functional groups in the coal samples increased significantly after acid washing. The O1s spectrum is divided into three peaks with different energies, i.e., 531.26 eV for phenol or ether (CO), 532 eV for carbonyl (*C=O), and 533 eV for carboxyl group (COO). SL contains more carboxyl groups; therefore, relative contents of phenols, ethers (*CO), and carboxyl groups (COO) in the coal samples obtained by pickling SL^+ and SL^{+2} increased significantly. These results are compatible with the results of FT-IR analysis, The oxygen-containing functional groups in lignite increased significantly after acid washing compared to water washing; however, acid washing led to the elimination of the inherent minerals from raw coal. Acid washing leads to the exposure of more oxygen-containing functional groups in the coal sample, which provides more sites for the formation of a coordination complex and hydrogen bonding for the coal sample to adsorb moisture.

3.1.4. Changes of Pore Structure in Coal Samples. The pore structure and other physical properties of lignite incur irreversible changes after treatment by various elution methods,[28] which significantly impacts the water-holding capacity of lignite. The N_2 adsorption method was employed to examine and compare the pore characteristics of raw coal and demineralized coal samples. The specific surface area and average pore diameter were both reduced slightly when the SL was demineralized step by step, as presented in Table 5. The specific pore volumes of SL^+ and SL^{+2} coal samples were significantly larger than those of other treatments. This is attributed to the fact that after the lignite pickling treatment, the macropores in the lignite particles get compressed, and thus they undergo collapse and clogging, resulting in a decrease in the specific surface of the lignite and at the same time a decrease in the average pore size.[29] Notably, the physical structure of lignite was more influenced by acid washing than by water washing.

3.1.5. Analysis of the Influence of Microstructure on the Interaction between Coal Samples and Water. After 24 h of water adsorption by coal samples, ^1H NMR spectroscopy was utilized to acquire the T_2 inversion spectra of SL and SL^{+2}, in which the relaxation time T_2 revealed the state and degrees of freedom of water. The signal peak in the T_2 relaxation inversion spectrum between 0.001−0.01 s was semibound water, whereas the signal peak between 0.01−0.1 s corresponded to free water.[30] A direct correlation was

https://doi.org/10.1021/acsomega.2c05786
ACS Omega 2023, 8, 9111−9120

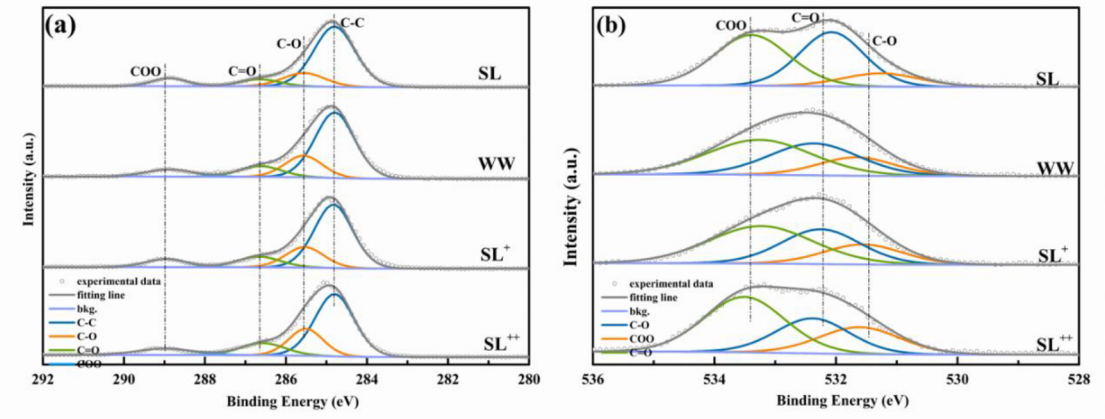

Figure 3. (a) XPS C1s spectra of coal samples, (b) XPS O1s spectra of coal samples.

Table 4. XPS O1s Spectrum Analysis of Shengli Raw Coal and Deashed Lignite

		content/%			
E/eV	oxygen form	SL	WW	SL^{+}	SL^{+2}
531.26	CO	12.34	17.86	19.17	23.55
532.07	C═O	42.05	35.96	33.35	27.97
533.39	COO	45.61	46.18	47.48	48.49

Table 5. BET Results of Shengli Raw Coal and Deashed Coal Samples

samples	specific surface area ($m^2 \cdot g^{-1}$)	average pore size (nm)	total pore volume × 10^{-3} ($cm^3 \cdot g^{-1}$)
SL	4.9845	0.0278	26.7019
WW	3.7013	0.0251	25.9801
SL^{+}	3.9459	0.0267	28.8477
SL^{+2}	4.1550	0.0257	27.5131
SL^{+2} - 50%	4.6344	0.0206	30.3165

observed between water mobility and the relaxation time of water and vice versa.[31] The two coal samples displayed main signal peaks in the range of 0.01−1 s after adsorbing moisture, as demonstrated in Figure 4, and the existing state of coal samples after the reabsorption of water was predominantly free

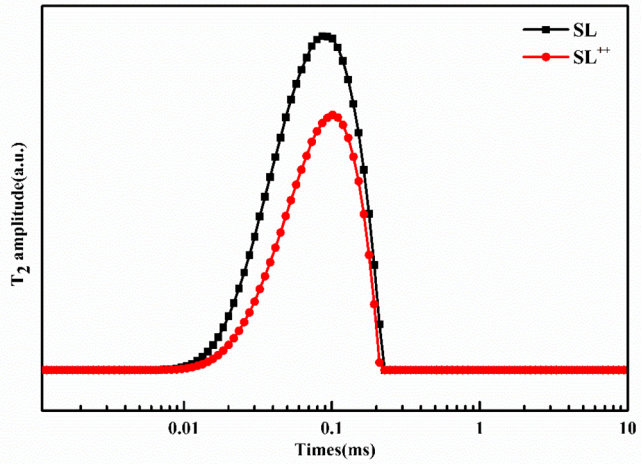

Figure 4. Moisture T_2 distribution diagram of the water adsorbed samples.

water. The relaxation time of SL^{+2} with the removal of intrinsic minerals shifted to the right compared to the main signal peaks of SL, revealing that the removal of intrinsic minerals reduced the interaction of the lignite−water molecules. The presence of inherent minerals in lignite enhances its capability to absorb moisture.

After stepwise acid washing, the changes in oxygen-containing functional groups, mineral ions, specific surface area, and EMCin the coal samples WW, SL^{+}, and SL^{+2} were compared and analyzed. The change rate in SL was calculated by comparing data on oxygen-containing functional groups, mineral ions, specific surface area, and equilibrium adsorption water content (Table 6). The mineral content of coal samples

Table 6. Change Rates of Oxygen-Containing Functional Groups, Minerals, Specific Surface Area, and Resorption Rate of Shengli Raw Coal and Deashed Coal Samples

samples	resorption rate/%	ash content/%	oxygen-containing functional groups/%	specific surface area/%
SL	0	0	0	0
WW	−6.99	−1.22	10.78	−25.74
SL^{+}	−31.57	−56.61	26.05	−20.84
SL^{+2}	−20.57	−93.35	39.57	−16.64

was favorably associated with the overall EMC, and $EMC_{SL++} > EMC_{SL+}$. The mineral content in SL^{+2} was produced by a significant reduction in minerals, increase in oxygen-containing functional groups, and increase in specific surface area, which leads to the moisture absorption of SL^{+2} more easily. This is the result of the interaction of inherent minerals, oxygen-containing functional groups and pores. The removal of intrinsic minerals led to a significant reduction in the hygroscopic performance of coal samples, while the more developed pore structure and exposure of the concentration of oxygen-containing functional groups on the surface of lignite improved the hygroscopic performance of coal samples.

3.2. Effect of Adding Spontaneous Combustion Residual Ash on Lignite Moisture Resorption. *3.2.1. Moisture Resorption Curve of Coal Samples with Externally Added Minerals.* It was found that Shengli lignite easily underwent spontaneous combustion after mining and aggregation in air, and the ash produced by the spontaneous combustion covered the lignite surface owing to environmental factors. Previously, it was observed that the step-by-step

https://doi.org/10.1021/acsomega.2c05786
ACS Omega 2023, 8, 9111−9120

demineralization of Shengli lignite might have influenced its hygroscopic performance. The removal of inherent minerals reduced the ability of lignite to absorb moisture, as evaluated by low-field NMR spectroscopy. To further characterize the influence of mineral ions on the moisture resorption performance of Shengli lignite, the impact of mineral ions on the lignite resorption performance after spontaneous combustion ashing was investigated herein. Water resorption experiments were performed on coal samples by introducing low-temperature spontaneous combustion ash from the outside, and the adsorption curve was plotted to explore the effect of ash after spontaneous combustion on its adsorption behavior.

TG and DTG curves of SL^{+2} and SL^{+2} - 50% are depicted in Figure 5. Coal samples SL^{+2} and SL^{+2} - 50% reduced a

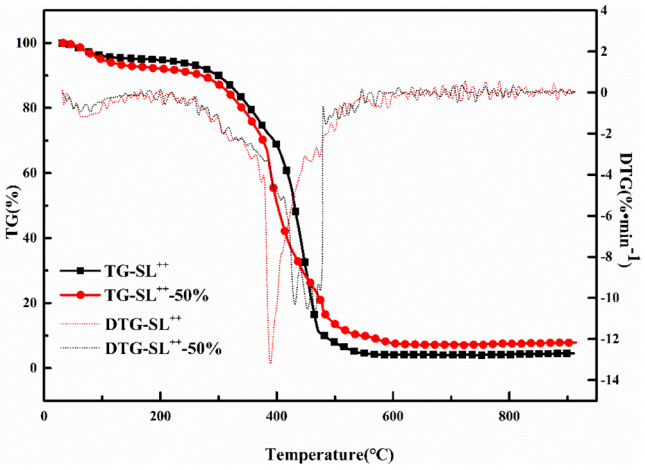

Figure 5. TG curves of treated coal samples.

significant portion of their weight in the range of 300−500 °C. Compared to SL^{+2}, the curve of SL^{+2} - 50% is shifted toward the low temperature region. Combining TG and DTG curves, the ignition point of SL^{+2} is 382.28 °C, and the ignition point of SL^{+2} - 50% is 337.97 °C, indicating that the incorporation of minerals into coal samples leads to an increase in the spontaneous combustion propensity, which is due to the combination of minerals and oxygen-containing functional groups in lignite to form a carboxylate structure, which promotes the combustion of coal samples. These results were consistent with a previous report.[32] Comparative analysis of the combustion residue from the TG curves indicates that the combustion residue of SL^{+2} - 50% was more than that of SL^{+2}, which is consistent with the mineral addition rule.

It was observed that when the hygroscopicity of the coal sample achieved equilibrium at a temperature of 30 °C and relative humidity of 43%, the residual ash of Shengli lignite exhibited a very low hygroscopicity (Figure 6(a)). However, the external addition of minerals to the SL^{+2} coal sample showed some effect on its hygroscopic ability (Figure 6(b)). Under the same humidity conditions, the trend of the EMC of coal samples after adding minerals was EMC_{SL++}-50% > EMC_{SL++}. The addition of a particular concentration of minerals can enhance the EMC of coal samples. This tendency is explained by changes in metal ions, oxygen-containing functional groups, and specific surface area in coal samples after exogenous mineral addition.

3.2.2. Changes of Minerals in Coal Samples with Externally Added Minerals. The discrete minerals in SL, SL^{+2}, and ash-added coal samples were evaluated via XRD, as displayed in Figure 7. The main constituents of Shengli lignite

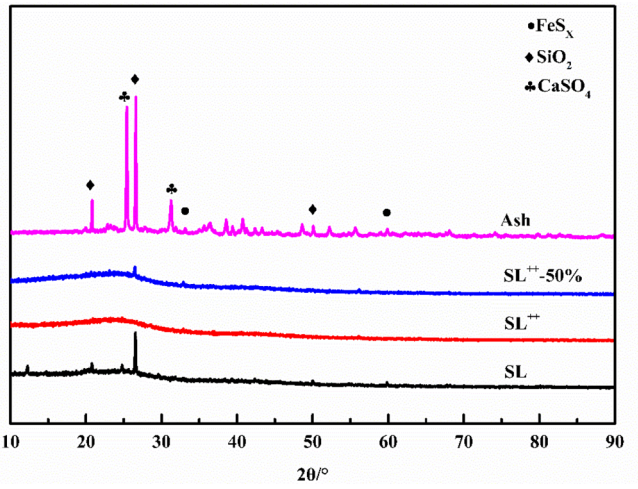

Figure 7. XRD patterns of raw coal and treated coal samples.

are quartz (SiO_2), kaolinite ($Al_4(OH)_8Si_4O_{10}$), and orthoclase ($K_4Al_4Si_{12}O_{32}$). All the diffraction peaks corresponding to quartz, kaolinite, and muscovite disappeared after the ash was eluted with HF. Shengli lignite is predominantly composed of

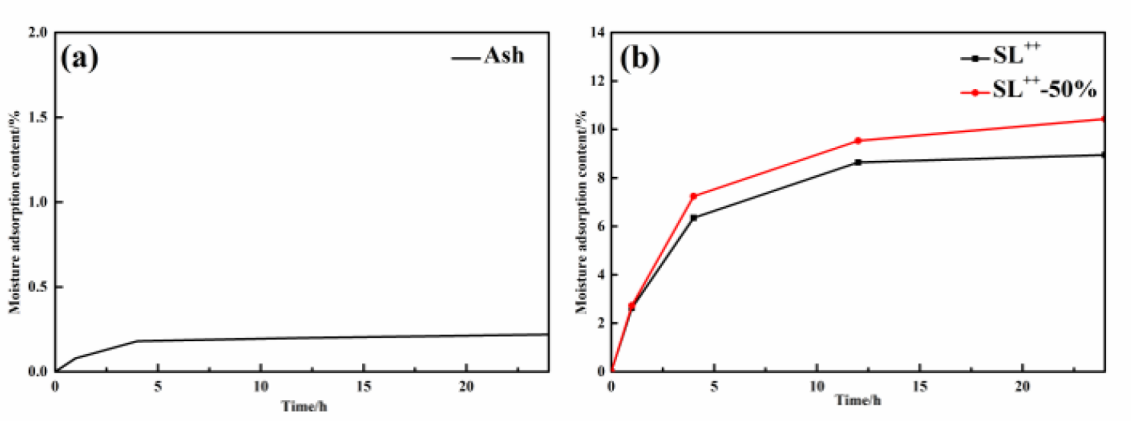

Figure 6. (a) Moisture adsorption curve of minerals; (b) moisture adsorption curve of coal samples with externally added minerals.

https://doi.org/10.1021/acsomega.2c05786
ACS Omega 2023, 8, 9111−9120

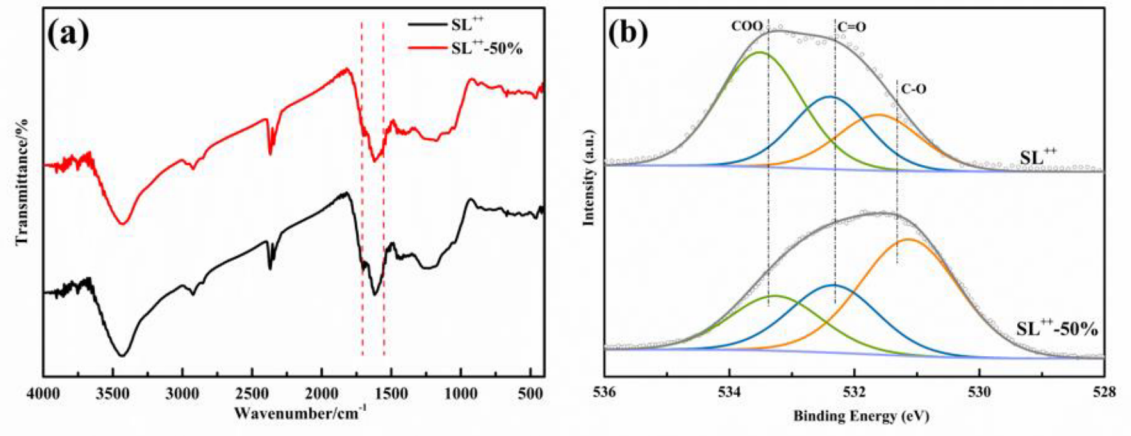

Figure 8. (a) FTIR spectra of treated coal samples; (b) XPS O1s spectra of treated coal samples.

metal oxides after spontaneous combustion and ashing. The crystal structure of the coal sample was different when it was introduced to SL^{+2}; only the diffraction peaks of quartz could be seen with that too with the weak peak intensity; and the diffraction peaks of mineral ions were not obvious. The ability of the coal sample to absorb water also changed slightly.

3.2.3. Changes of Oxygen-Containing Functional Groups in Coal Samples with Externally Added Minerals. The FTIR spectroscopy and XPS analysis were performed for SL^{+2} and mineral-added coal samples. Figure 8(a) depicts the changes in oxygen-containing functional groups in coal samples, and the peak fitting of oxygen-containing functional groups O1s is shown in Figure 8(b). The stretching vibration was enhanced for SL^{+2}- 50% in the range of 450−1200 cm^{-1}, which belonged to the distinct mineral peaks. Valence bond vibrations of C−O, C−O−C, and −COOH groups were observed at 1100−1300 cm^{-1} and 1708 cm^{-1}. The stretching vibration of SL^{+2}- 50% was weaker than that of SL^{+2}, which was possible because of the fact that a portion of ash and oxygen-containing functional groups on the surface of lignite experienced ion exchange, resulting in the weakening of oxygen-containing functional groups and formation of more [−(COO)nX] structures in the coal sample. SL^{+2} - 50% also exhibited enhanced aliphatic absorption peaks at 2990−2800 cm^{-1}. Figure 8(b) shows that the relative content of SL^{++} - 50% carboxyl group (−COO) decreased obviously, while the relative content of C−O functional group increased significantly, indicating that addition of mineral to coal increased the number of aliphatic functional groups. The oxygen-containing functional groups of SL^{+2} exhibited the highest stretching vibration; however, the EMC was lower than that of SL^{+2} - 50%.

3.2.4. Changes in the Physical Structure of Coal Samples with Externally Introduced Minerals. Moreover, the inclusion of minerals also influences the physical properties of the coal samples, such as pore structure. The N_2 adsorption method was employed herein to compare the pore properties of the treated coal samples, as presented in Table 5. Compared to SL^{+2}, the specific surface area and pore volume of SL^{+2} - 50% were dramatically increased; nonetheless, the average pore size got relatively reduced. This was because the minerals added to the surface of the coal sample enhanced the specific surface area and pore volume of coal sample. Some minerals entered the pores of the coal sample and clogged the pore space.

3.3. Analysis of the Influence of External Minerals on the Interaction between Coal Samples and Water. The T_2 inversion spectra of SL^{+2} and SL^{+2} - 50% were obtained by ^1H NMR spectroscopy after 24 h of water adsorption. Among them, the relaxation time T_2 revealed the state and degree of freedom of water, while the peak area indicated the water content in different states. Figure 9 illustrates that the change

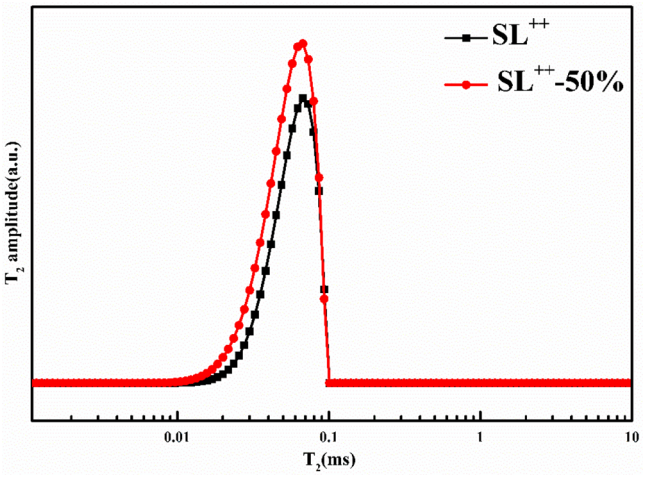

Figure 9. T_2 distribution diagram of treated coal samples.

in the moisture signal peak is mainly concentrated at T_2 (0.01−0.1 s). There is only one peak in the inversion spectrum of the moisture change of the four coal samples in the figure, which corresponds to the free water range based on the relaxation time.[33] The T_2 inversion spectra of the moisture change varied for different coal samples with the same adsorption time. According to the T_2 inversion spectrum, the peak area of SL^{+2} - 50% is significantly larger than that of SL^{+2}, as well as its signal peak shifts leftward, indicating that the binding force of coal sample with water is stronger and the moisture adsorption capacity of SL^{+2} - 50% is enhanced. Furthermore, the results indicate that a particular quantity of minerals added to the coal sample interacts with the water clusters, enhancing the binding force of the water molecules on the coal surface, which is in good agreement with the viewpoint and results presented in a previous study.[21]

3.4. Mechanism of Enhanced Mineral Interaction with Coal−Water Molecules. According to the theory of lignite moisture adsorption, the water absorption of lignite is mainly influenced by oxygen-containing functional groups. The

https://doi.org/10.1021/acsomega.2c05786
ACS Omega 2023, 8, 9111−9120

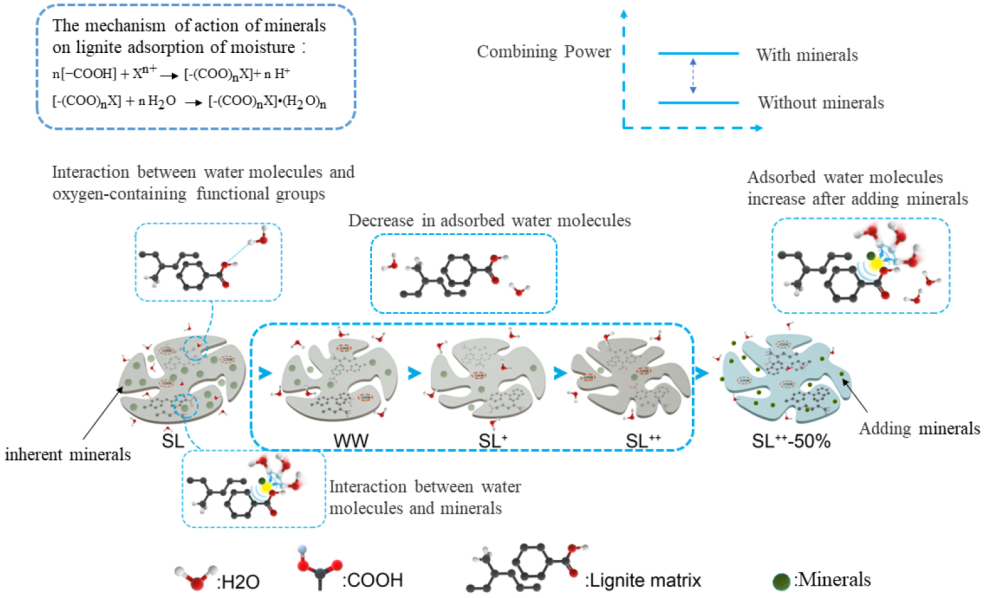

Figure 10. Mechanism diagram of the enhancement of lignite−water interaction by minerals.

greater the number of hydrophilic oxygen-containing functional groups on the lignite surface, the denser the polar sites, and the easier it is to attract water molecules, in particular, for the extremely polar acidic oxygen-containing functional groups.[34]

Overall, the promoting mechanism of minerals in the process of lignite adsorption of water molecules was proposed. Presumably, the intrinsic minerals and the externally introduced mineral components were uniformly dispersed in the main structure of the lignite macromolecular skeleton. The adsorption of moisture by lignite occurred in the following two stages: single-layer adsorption and multilayer adsorption. When the coal sample was moistened, water molecules were preferentially adsorbed on the surface of coal particles with strong hydrophilicity and coupled with polar groups to develop single-molecule adsorption, and subsequently, more water molecules were adsorbed for multilayer adsorption. For the step-by-step demineralization treatment of lignite, water washing can wash away the soluble minerals present in the coal samples, and the slight reduction in the specific pore volume of the coal sample can expose part of the oxygen-containing functional groups on the surface of the lignite. The content of C−O and COOH increases, the content of C═O decreases, the structure of [(COO)nX] in coal sample decreases, and the interaction force between lignite and water molecules decreases. Compared to water washing, HCl washed away some HCl-soluble minerals, and the specific pore volume of the coal sample increased substantially, exposing more oxygen-containing functional groups on the surface of lignite, and the contents of C−O and COOH increased; however, the moisture absorption capacity of the coal sample was impaired. HCl/HF is more effective at removing minerals. Due to the significant reduction of mineral ions, and the pore structure of the coal sample became more developed. The oxygen-containing functional groups on the surface of the coal sample were exposed more, in which the [-(COO)nX] structure is exchanged with H^+ to form COOH. Compared to the HCl-washed coal sample, this coal sample absorbed more moisture because mineral ions were enhanced, the interaction force between SL^{+2} and water molecules is obviously weakened (Figure. 4), and the EMC content of coal samples also decreases. Adding spontaneous combustion ashing to the SL^{+2} coal sample, the content of mineral ions in the coal sample increases, minerals entered the pores of the coal sample and clogged the pore space and increases the specific surface area of coal samples, decreases the COOH content in coal samples, forms more [-(COO)nX] structures with metal ions, strengthens the interaction force between lignite and water molecules (Figure 9), and also increases the EMC content of coal samples. Because mineral ions enhanced the specific surface area of lignite and occluded a portion of the pores in coal samples. On the other hand, they coupled with oxygen-containing functional groups on the surface of lignite, in particular, carboxyl functional groups, which are abundant in lignite and are capable of forming two hydrogen bonds with water molecules, to form intermediate complexes. As a result, more [-(COO)nX] structures are formed, which thus enhances the action strength of lignite's polar points. Consequently, the interaction force between lignite and water molecules increases. When the spatial distance between the hydrophilic sites is small enough, water molecules can establish hydrogen bonds with multiple hydrophilic sites, attaining a stable structure to produce water clusters, adsorbing more water molecules, and forming a more stable adsorption layer in the state of multilayer adsorption of water as confirmed by prior studies as well.[10,23,27]

4. CONCLUSIONS

In this study, the impacts of removing inherent minerals from lignite and introducing spontaneous combustion residual ash on the moisture resorption performance of coal samples were investigated systematically from three perspectives: pore structure, oxygen-containing functional groups, and minerals. The modifications in lignite−water molecules interactions during mineral removal were investigated by low-field NMR spectroscopy. The inherent mineral content of lignite got dramatically reduced after a step-by-step demineralization treatment, and the equilibrium adsorption water content of the coal samples showed a trend of $EMC_{SL} > EMC_{WW} > EMC_{SL++} > EMC_{SL+}$. Mineral content was overall positively correlated

https://doi.org/10.1021/acsomega.2c05786
ACS Omega 2023, 8, 9111−9120

with EMC, except in SL^{+2}, where the mineral content decreased sharply, oxygen-containing functional groups increased, and the specific surface area increased, resulting in $EMC_{SL++} > EMC_{SL+}$ due to the combined action of inherent minerals, oxygen-containing functional groups, and pores. Simultaneously, the removal of inherent minerals in the lignite sample caused the relaxation time of the coal sample to shift to the right, indicating that the removal of minerals reduced the interaction of the lignite−water molecules. The EMC of lignite residual ash from spontaneous combustion was approximately zero. However, after mixing with lignite, it coupled with the oxygen-containing functional groups on the surface of lignite and promoted the adsorption of water molecules in lignite. This led to the increase in the EMC of SL^{+2} and enhancement in the interaction force between lignite and water molecules, causing the relaxation time of coal samples to shift to the left. In general, inherent and exogenous minerals coupled with oxygen-containing functional groups on the lignite surface form intermediate complexes, enhancing the action force of polar sites and the interaction force between lignite and water molecules.

AUTHOR INFORMATION

Corresponding Author

Yue Yin Song − *College of Chemical Engineering, Inner Mongolia University of Technolegy, Huhhot 010051, China*; Email: songyueyin@163.com

Authors

Ying Yue Teng − *College of Chemical Engineering and Inner Mongolia Key Laboratory of High-Value Funtional Utilization of Low Rank Carbon Resources, Inner Mongolia University of Technolegy, Huhhot 010051, China*; orcid.org/0000-0001-7690-8355

Shi Rui Han − *College of Chemical Engineering, Inner Mongolia University of Technolegy, Huhhot 010051, China*

Xue Bai − *College of Chemical Engineering, Inner Mongolia University of Technolegy, Huhhot 010051, China*

Yin Min Song − *College of Chemical Engineering and Inner Mongolia Key Laboratory of High-Value Funtional Utilization of Low Rank Carbon Resources, Inner Mongolia University of Technolegy, Huhhot 010051, China*; orcid.org/0000-0003-0667-7760

Complete contact information is available at: https://pubs.acs.org/10.1021/acsomega.2c05786

Notes

The authors declare no competing financial interest.

ACKNOWLEDGMENTS

This work was supported by the National Natural Science Foundation of China (21766023), the Plan of Science and Technology of Inner Mongolia (2019GG268), the Science Foundation of Inner Mongolia Technology University (ZZ201906), and the Scientific Research Project for Higher Education Institution of Inner Mongolia (NJZY21150).

REFERENCES

(1) Zhang, S. Q. Practice and prospect of clean and efficient utilization of coal in China. *J. Science and Technology Rev.* **2016**, *34*, 56−63. In Chinese.

(2) Zhao, Q. Clean and and efficient utilization of Lignite resources in China. *J. Clean Coal Technol. (Beijing, China)* **2018**, *24*, 9−14.

(3) Feng, L.; Yuan, C.; Mao, L.; Yan, C.; Jiang, X.; Liu, J.; Liu, X. Water occurrence in lignite and its interaction with coal structure. *J. Fuel.* **2018**, *219*, 288−295.

(4) Xia, W. C.; Xie, G. Y.; Peng, Y. L. Recent advances in beneficiation for low rank coals. *J. Powder Technol.* **2015**, *277*, 206−221.

(5) Nikolopoulos, N.; Violidakis, I.; Karampinis, E.; Agraniotis, M.; Bergins, C.; Grammelis, P.; Kakaras, E. Report on comparison among current industrial scale lignite drying technologies (A critical review of current technologies). *J. Fuel* **2015**, *155*, 86−114.

(6) Qu, Z.; Sun, F.; Gao, J.; Pei, T.; Qie, Z.; Wang, L.; Pi, X.; Zhao, G.; Wu, S. A new insight into the role of coal adsorbed water in low-temperature oxidation: Enhanced·OH radical generation. *J. Combust. Flame* **2019**, *208*, 27−36.

(7) Norinaga, K.; Kumagai, H.; Hayashi, J. I.; Chiba, T. Classification of water sorbed in coal on the basis of congelation characteristics. *J. Energy Fuels* **1998**, *12*, 574−579.

(8) Fei, Y.; Chaffee, A.; Marshall, M.; Jackson, W. R. Lignite-water interactions studied by phase transition-differential scanning calorimetry. *J. Fuel* **2005**, *84*, 1557−1562.

(9) Feng, L.; Yuan, C. Z.; Mao, L. Z.; Yan, C. Y.; Jiang, X. G.; Liu, J.; Liu, X. C. Water occurrence in lignite and its interaction with coal structure. *J. Fuel* **2018**, *219*, 288−295.

(10) Liu, J.; Jiang, X. G.; Cao, Y.; Zhang, C.; Zhao, G. Y.; Zhao, M. S.; Feng, L. Exploring the effect of oxygen-containing functional groups on the water-holding capacity of lignite. *J. Mol. Model.* **2018**, *24*, 130−140.

(11) Xiao, J.; Zhao, Y. P.; Fan, X.; Cao, J. P.; Kang, G. J.; Zhao, W.; Wei, X. Y. Hydrogen bonding interactions between the organic oxygen/nitrogen monomers of lignite and water molecules: A DFT and AIM study. *J. Fuel Process. Technol.* **2017**, *168*, 58−64.

(12) Liu, X. Y.; Liu, S. Y.; Fan, M. Q.; Zhang, L. Decrease of hydrophilicity of lignite using CTAB: Effects of adsorption differences of surfactant onto mineral composition and functional groups. *J. Fuel* **2017**, *197*, 474−481.

(13) Han, Y. N.; Bai, Z. Q.; Liao, J. J.; Bai, J.; Dai, X.; Li, X.; Xu, J. L.; Li, W. Effects of phenolic hydroxyl and carboxyl groups on the concentration of different forms of water in brown coal and their dewatering energy. *J. Fuel Process. Technol.* **2016**, *154*, 7−18.

(14) Wei, F. J.; Liao, J. J.; Chang, L. P.; Han, Y. N.; Bao, W. R. Transformation of functional groups during lignite heat-treatment and its effects on moisture re-adsorption properties. *J. Fuel Process. Technol.* **2019**, *192*, 210−219.

(15) Zhang, Y. L.; Jing, X. X.; Jing, K. G.; Chang, L. P.; Bao, W. R. Study on the pore structure and oxygen-containing functional groups devoting to the hydrophilic force of dewatered lignite. *J. Appl. Surf. Sci.* **2015**, *324*, 90−98.

(16) Bai, X.; Song, Y. Y.; Teng, Y. Y.; Zhang, W. L.; Song, Y. M.; Wang, Y. F. Effect of -O- on Water Molecule Adsorption and AdsorptionMechanism of Lignite and Coke. *J. J. Chem.* **2021**, *2021*, 1.

(17) Yang, Y. L.; Jing, X. X.; Li, Z. Q.; Liu, X.; Zhang, Y. L.; Chang, L. P. Effect of drying conditions on moisture re-adsorption performance of dewatered lignite. *J. Drying Technol.* **2013**, *31*, 1430−1437.

(18) Feng, X. F.; Zhang, C.; Tan, P.; Zhang, X. P.; Fang, Q. Y.; Chen, G. Experimental study of the physicochemical structure and moisture readsorption characteristics of Zhaotong lignite after hydrothermal and thermal upgrading. *J. Fuel* **2016**, *185*, 112−121.

(19) Gosiewska, A.; Drelich, J; Laskowski, J. S.; Pawlik, M. Mineral matter distribution on coal surface and its effect on coal wettability. *J. J. Colloid Interface Sci.* **2002**, *247*, 107−116.

(20) Liu, X. C. Forms of water in Shengli lignite and effect of metal ions on its water absorption capacity. *D. China University of Mining and Technology* **2014**. In Chinese.

(21) Shang, X. L.; Hou, K.; Wu, J. J.; Zhang, Y. X.; Liu, J. Q.; Qi, J. The influence of mineral matter on moisture adsorption property of Shengli lignite. *J. Fuel* **2016**, *182*, 749−753.

(22) Fei, Y.; Giroux, L.; Marshall, M.; Jackson, W. R.; Macphee, J. A.; Charland, J. P.; Chaffee, A. L. A comparison of primary lignite

https://doi.org/10.1021/acsomega.2c05786
ACS Omega 2023, 8, 9111−9120

structure as determined by pyrolysis techniques with chemical characteristics determined by other methods. *J. Fuel* **2006**, *85*, 998−1003.
(23) Liu, X. C.; Feng, L.; Wang, X. H.; Zhang, Y.; Tang, H. Y. Effect of Mg^{2+} content in ion-exchanged Shengli lignite on its equilibrium adsorption water content and its mechanism. *J. Chin. J. lChem. Eng.* **2015**, *23*, 456−460.
(24) Su, H. X. An experimental study on the existing form of water in lignite. *D. Liaoning University of Science and Technology* **2014**. In Chinese.
(25) Liu, L. H. Effect of thermal upgrading on characteristics of moisture re-adsorption and spontaneous combustion for low rank coal. *D. China University of Mining and Technology (Beijing)* **2017**. In Chinese.
(26) Wei, Q.; Tang, Y. G.; Li, W. W.; Zhao, Q. J.; He, X.; Li, L.; Zhao, Z. F. Research advances on organic sulfur structures in coal. *J. J. China Coal Soc.* **2015**, *40*, 1911−1923.
(27) Laudal, D. A.; Benson, S. A.; Addleman, R. S.; Palo, D. Leaching behavior of rare earth elements in fort union lignite coals of North America. *J. Int. J. Coal Geol.* **2018**, *191*, 112−124.
(28) Huang, B.; Liu, G. W.; Wang, P. H.; Zhao, X.; Xu, H. X. Effect of nitric acid modification on characteristics and adsorption properties of lignite. *J. Processes* **2019**, *7*, 167−183.
(29) Zhu, X. Q.; Tian, J. P.; Liu, Y.; Chen, Z. S.; Miao, Z. Y.; He, Q. Q. Effect of acid treatment on the structure of Mengdong lignite. *J. Coal. Eng. (China)* **2018**, *50*, 137−141.
(30) Song, P.; Peng, Y. F.; Wang, G. H.; Song, P.; Wang, K. T.; Yang, T. Detection of internal water flow in germinating corn seeds based on low field nuclear magnetic resonance. *J. Trans. Chin. Soc. Agric. Eng.* **2018**, *34*, 274−281.
(31) Xin, Y.; Zhang, M.; Adhikari, B. Effect of trehalose and ultrasound-assisted osmotic dehydration on the state of water and glass transition temperature of broccoli (Brassica oleracea L. var. botrytis L.). *J. J. Food Eng.* **2013**, *119*, 640−647.
(32) Yan, Z. H.; Chen, J. M.; He, R. X.; Li, N.; Zhou, H. C.; Song, Y. M.; Ban, Y. P.; Zhi, K. D.; Teng, Y. Y.; Liu, Q. S. Suppression of crosslinking combination of carboxyl functional groups with NaOH on combustion performance of Shengli lignite. *J. Fuel* **2018**, *227*, 13−20.
(33) Wang, X. Y.; Wei, Z. C.; Sun, C. Z.; Zhang, L. L. Moisture transfer characteristic of carrot slices by infrared radiation drying. *J. Trans. Chin. Soc. Agric. Mach.* **2015**, *46*, 240−245.
(34) Zheng, J. X.; Xu, Z. Q.; Ren, Y. G.; Zhang, Y. X.; Cao, Z. N.; Xue, J. F. Effects of petroleum coke on re-adsorption characteristics of lignite upgraded by microwave. *J. Coal. Eng. (China)* **2018**, *50*, 134−139.

https://doi.org/10.1021/acsomega.2c05786
ACS Omega 2023, 8, 9111−9120